1965

The elastic and anelastic constants of a synthetic fluor-mica formed by glass-ceramic fabrication techniques

John H. Ainsworth

Department:

THE ELASTIC AND ANELASTIC CONSTANTS OF A SYNTHETIC FLUOR-MICA FORMED BY GLASS-CERAMIC FABRICATION TECHNIQUES

by

JOHN H. AINSWORTH

A

THESIS

submitted to the faculty of the

UNIVERSITY OF MISSOURI AT ROLLA

in partial fulfillment of the requirements for the

Degree of

MASTER OF SCIENCE IN CERAMIC ENGINEERING

Rolla, Missouri

1965

Approved by

R. E. Moore (Advisor) D. L. Branson

D. R. Edwards John V. Mayo

ABSTRACT

A tetrasilicic fluor mica, $K_2Mg_5Si_8O_{20}F_4$, was synthesized using glass forming techniques. Density changes, weight losses, and shrinkage, as well as elastic and anelastic properties, were measured on bars heat-treated at selected temperatures between 500°C and 1150°C to determine the characteristics of this material. Phase changes were followed by determining thermal expansion, logarithmic decrement, and modulus of elasticity from room temperature to 800°C.

It was found that the elastic and anelastic constants decreased gradually with heat treatments from 600°C to 1000°C. This indicated progressively increased structural ordering. Heat treatments above 1000°C produced appreciable decreases in the elastic constants and equally appreciable increases in the anelastic constants. This was evidence of increasing mica crystal growth. Determinations of the modulus of elasticity, logarithmic decrement, and thermal expansion from room temperature to 800°C showed the transformation from an amorphous to ordered structure to occur at 600°C. There was also an indication of ionic arrangement prior to the actual transformation.

ACKNOWLEDGEMENTS

The author wishes to express his gratitude to his advisor, Dr. Robert E. Moore, for his support and encouragement, and also to Dr. D. E. Day and Prof. G. E. Lorey for their many valuable suggestions.

The financial assistance of the Advanced Electronics Division, Litton Corporation in the form of a fellowship and research fund is greatly appreciated.

To my dear wife, Alice, I can only say thank you for your continued support, encouragement, and understanding.

TABLE OF CONTENTS

LIST OF FIGURES

LIST OF TABLES

I. INTRODUCTION

Mica is a mineral of considerable economic value; it is unique in its combination of properties useful in industry. Perfect cleavage, transparency, flexibility, non-conductivity of heat and electricity, resistance to high temperatures, and resistance to chemical decomposition constitute an assemblage of properties possessed by no other single mineral. One or more of these properties has led to the increased use of mica, which is now indispensable in the electrical and electronics industries.

Because of the strategic importance of certain natural micas, increased attention has been directed toward the synthesis of micas which could be used as substitutes. It has been demonstrated[1] that micas having extremely useful properties can be synthesized by melt crystallization and solid-state reaction. Micas having excellent dielectric properties have been made by hot-pressing techniques. Phosphate-bonded mica has proven promising, although inferior to hot-pressed mica.

Glass-ceramic processes have recently been explored by several investigators[2,3] as a possible method of synthesizing mica. Tuzzeo[3], while a graduate student at the University of Missouri, School of Mines and Metallurgy, made substantial progress in the development of a tetrasilicic fluor-mica dielectric by glass-ceramic fabrication techniques. He was able to form glass disks and rods, and by subsequent heat treatments at selected temperatures between 620°C and 1160°C obtained varying degrees of devitrification within the glass. Using density changes as a correlation to crystal content, Tuzzeo reported maximum crystal yields of 86 weight percent.

The purpose of the present investigation was to employ elastic and anelastic measurements, determined by sonic vibration techniques, to gain insight into the crystallization kinetics of the tetrasilicic fluor-mica glass-ceramic. Furthermore, through these studies, it was hoped to determine the capabilities and sensitivity of sonic elastic and damping measurements as an experimental tool for following structural changes in a glass-ceramic.

II. REVIEW OF LITERATURE

A. Classification of Mica

The name mica is applied to a large group of minerals, all of which are complex silicates of various metals. Dana[4] has classified four principal types of mica, each having several varieties. These classifications are:

Biotite	$K_2(Mg,Fe)_6Al_2Si_6O_{20}(OH)_4$
Muscovite	$K_2Al_6Si_6O_{20}(OH)_4$
Phlogopite	$K_2Mg_6Al_2Si_6O_{20}(OH)_4$
Lepidolite	$K_2Li_4Al_2Si_8O_{20}(OH)_4$

The precise formulas and isomorphic relations of the different mica varieties have been subject to much study. Winchell's[5,6] investigations of mica led to two general classifications: the heptaphyllites, characterized by a seven atom molecule, and the octaphyllites, characterized by an eight atom molecule. Following this classification, biotite and phlogopite belong in the octaphyllites, whereas, muscovite and lepidolite are heptaphyllites. Winchell noted that no solubility was ever evidenced between the two systems; thus once chemically analyzed, a mica can be classified definitely in one of the two systems. It was also noted that in nearly all cases an octaphyllite has the optic plane parallel to 010 while a heptaphyllite has the optic plane perpendicular to 010.

Pauling[7] proposed a general formula for micas on the basis of structural considerations and coordination theory. This formula is:

$$KX_nY_4O_{10}(OH,F)_2,$$

where $2 \leq n \geq 3$,

X = cations of coordination number 6, and

Y = cations of coordination number 4.

Stevens[8] argued that Winchell's classification was complex and of limited application. He thus proposed that micas be classified as dioctrahedral or trioctrahedral. The dioctrahedral micas have 2/3 of their octrahedral positions filled while the trioctrahedral micas have all their octrahedral positions filled. Stevens was further able to express the compositions of micas in percentages of comparitively simple end-member formulas which satisfied the chemical and structural requirements of mica.

B. Mica Synthesis

In the United States, extensive efforts on mica synthesis have been carried out by the United States Bureau of Mines[1] Electrotechnical Laboratory, Norris, Tennessee. Objectives of this work included studies of fluorine micas and production of synthetic mica sheets by melt crystallization on a pilot plant scale. The major objective, mica sheets greater than two to three inches square, was never obtained; however, valuable information was gained from this work. It was demonstrated that hundreds of mica compositions could be prepared by melt crystallization or solid-state reaction, and that physical properties could be controlled by mica composition. The most satisfactory containers for melt crystallization included platinum, graphite, high silica fireclay, and silicon carbide. In cooperation with the Integrated Mica Corporation, it was found that sheet mica could be made successfully by mechanically disintegrating synthetic mica flakes and reintegrating the small flakes by modified paper making processes.

Limitations on the synthetic micas were observed during these studies. Under humid conditions, the synthetic mica had a tendency

to defluorinate and decompose above 800°C. The chief fault seemed to be that the synthetic micas contained glass and magnesium fluoride which were deleterious to the mechanical and dielectric properties.

Although melt crystallization techniques were not entirely successful, hot-pressing synthetic micas appeared promising. It was found that a strong, uniform, hot-pressed ceramic, showing little evidence of preferred orientation, could be made from mica previously synthesized by solid-state reaction. Several of these micas had good to excellent electrical insulating properties at both room temperature and elevated temperatures.

Because of the expense involved in hot-pressing, other methods of fabrication were investigated. Phosphate-bonding studies were conducted on three fluorine-mica compositions: $K_2Mg_6Al_2Si_6O_{20}F_4$, $K_4Mg_6B_2Si_6O_{20}F_4$, and $K_2Mg_5Si_8O_{20}F_4$. Physical characteristics were found to vary with the amount of orthophosphoric acid used for bonding, the compacting pressure, and the firing temperature. Dielectric properties were inferior to those of the hot-pressed mica.

Of special interest to the present work, was the brief study made on fused-cast mica ceramics. It was demonstrated that the tetrasilicic mica, $K_2Mg_5Si_8O_{10}F_4$, was best suited for this technique. Because of forming problems, however, this method was not investigated extensively.

C. Glass-Ceramics

A growing interest has followed the recent findings that certain glasses containing nucleating agents may be formed, cooled, and later crystallized to fine-grained ceramics with useful properties. Glass-ceramics have the advantages of low cost processing, reproducibility,

and a uniform structure approaching an ideal polycrystalline structure.

Stookey[9] has noted that glass-ceramics present new problems; however, they also provide solutions to many difficulties associated with conventional sintered ceramics. Porosity, which is detrimental to the strength, acid resistance, and high thermal conductivity of ceramics, is eliminated by making articles of glass-ceramics. Also, making articles of fine-grained glass-ceramics permits the use of anisotropic crystals, i.e., crystals having different properties along different crystallographic axis. Anisotropy in larger grained sintered ceramics causes porosity and mechanical weakness; whereas, in the smaller grained glass-ceramics, anisotropy has not been observed to induce this weakening effect to as great a degree.

Sintered ceramics and glass-ceramics each follow very different reaction paths. The sintering process starts with crystals already present. These either remain stable throughout the sintering cycle or undergo solid-state reactions. Thus, the composition and microstructure of the final product are influenced by these initial crystals. On the other hand, a glass contains its ionic constituents in essentially random distribution. Its crystallization kinetics can be decisively affected by the nucleating agent and other factors that influence molecular organization. Therefore, the crystal size and shape of a glass-ceramic may be entirely different from a sintered ceramic of the same composition.

The crystallization of most glass-ceramics is a two-stage process: the nucleation of the crystal phase and the subsequent growth of the crystals. It has been stated[10] that the nucleation is the most crucial

step.

Stookey[11] successfully used catalysts to form nucleation sites for crystallization. The glass article was first cooled and later reheated to a temperature range where the catalyst crystal was homogeneously nucleated to become the heterogeneous nucleation site for the crystal phase.

A second mechanism used to describe nucleation has been suggested by Stookey and Maurer[10]. This consists of a liquid-liquid unmixing within the glass which gives rise to the heterogeneous nucleation of the crystal phase.

Hillig[12], in studies of the ternary system $BaO-SiO_2-TiO_2$, and the quaternary system $BaO-Al_2O_3-SiO_2-TiO_2$, concluded that heterogeneous nucleation catalysis is not essential for uniform devitrification. He proposed that the precipitate structure results from a homogeneous nucleation process, i.e., one that is intrinsic to the system.

Until quite recently, it was felt that only "special" glasses could be nucleated by glass-ceramic techniques. However, studies[13] on a glass composition very similar to commercial soda-lime-silica glass have revealed phase separation. The miscibility temperature was established at 750°C. It was further determined that phase separation would not occur unless the thermal history of the glass included a time period below 701°C. Determination of growth rate at 660°C indicated the growth to be diffusion controlled. The significance of this work is that it is quite possible to place a glass-ceramic of low cost composition on the market. Furthermore, forming equipment is available and proven.

D. Glass-Ceramic Micas

Chen[2] investigated the kinetics of a synthetic phlogopite glass-mica. He found crystallization to occur as a two-stage process. In the range of 720°C to 760°C, an intermediate pseudocrystalline phase developed. The mica crystals initially formed at the interfaces of the pseudocrystalline phase and the glass phase; subsequent growth was within the pseudocrystalline phase. The maximum crystal formation was found to occur at 1000°C.

In a recent study, Tuzzeo[3] synthesized a tetrasilicic mica ($K_2Mg_5Si_8O_{20}F_4$) by glass-ceramic fabrication techniques. Density measurements were used for quantitatively determining the crystal content. From these data, Tuzzeo reported crystallinities of greater than 70 weight percent by heat treatments above 800°C; a maximum crystal yield of 86 weight percent was obtained with a heat treatment of 1000°C for three hours. Appreciable density changes at temperatures between 500°C and 630°C led to speculation that crystal nucleation and growth might occur at temperatures as low as 500°C. Tuzzeo reported considerable differences in microstructure of specimens heat-treated at 1100°C for three hours and twelve hours respectively. The three hour heat treatment yielded small, regularly shaped crystals; whereas, the twelve hour heat treatment produced larger, irregularly shaped mica crystals. Also, heat treatments above 1000°C produced decreases in density. This was felt to be caused by resorption of the crystal phase.

E. Measurement of Elastic Constants

1. Relations Between Young's Modulus and Flexural Vibrations

It is well known that the natural frequency of vibration of a

material is a quantity which may be used to determine Young's modulus of elasticity. For flexural vibration, this relation has been given[14] as:

$$f_n = \frac{K^2 m}{2L^2} \sqrt{E/d} \quad , \qquad (1)$$

where K = radius of gyration,

L = Length,

d = density,

E = modulus of elasticity,

f_n = natural frequency, and

m = constant depending upon mode of vibration.

Rayleigh[14] has shown the constant m to be:

4.7300408 for the first mode of vibration,

7.8532046 for the second mode of vibration, and

10.9955743 for the third mode of vibration.

By rearrangement of equation 1, the modulus of elasticity may be found directly as:

$$E = \frac{4\pi^2 L^4 f_n^2 d}{K^2 m^4} \cdot \qquad (2)$$

In the above equation, the effects of shear, lateral inertia, and rotary inertia have been neglected. These effects have been taken into consideration by other investigators. Timoshenko[15] corrected for shear and rotary inertia, whereas, Mason[16] and Thomson[17] corrected for lateral inertia and rotary inertia.

Pickett[18] established the most satisfactory solution. He corrected and simplified Goen's work which was based on Timoshenko's differential equation for transverse vibrations in a bar. This equation is of the form:

$$E = \frac{4\pi^2 L^4 f_n^2}{K^2 m^4} \, d \, .(T). \qquad (3)$$

The term T is Goen's correction factor depending upon the ratio of thickness to length, Poisson's ratio, and a shear constant which Pickett has shown to be approximately 5/6. Pickett gave algebraic equations relating T to K/L for Poisson's ratio (u) equal to 0, 1/6, and 1/3. In addition, he gave numerical solutions of these equations and graphs based on these solutions.

Spinner et. al.[19] used a quadratic interpolation from Pickett's equations for u = 0, 1/6, and 1/3 to obtain values of T for different values of Poisson's ratio. APPENDIX A gives equations for T as given by Spinner and Pickett.

2. Relation Between Shear Modulus and Torsional Vibrations

The shear modulus as a function of torsional frequency can be calculated by use of the following equation[18]:

$$G = \frac{4LR}{gAi^2} \, W(n')^2, \qquad (4)$$

where n' = torsional frequency,

A = cross sectional area,

i = unity for the first mode, two for second mode, etc.,

R = ratio of polar moment of inertia to the shape factor for torsional rigidity.

Pickett[18] states that the ratio R is unity for circular cross sections and 1.183 for square cross sections. For rectangular sections, R can be computed by use of the formula:

$$R = \frac{a/b + b/a}{4a/b - 2.52(a/b)^2 + 0.21(a/b)^6}, \qquad (5)$$

where a = thickness of bar and

b = width of bar.

3. Dynamic Techniques for Determining Elastic Constants

The elastic constants of a material are often determined by dynamic techniques. Numerous investigators[20,21,22] have described these techniques. Briefly, a signal from a variable frequency audio oscillator is amplified and fed to an electromagnetic driver, usually a phonograph cutting head or speaker, which in turn mechanically vibrates the specimen being tested. As resonance is reached, the increased amplitude of vibrations of the specimen is detected by a quartz pick-up resting lightly on the specimen. The signal from the pick-up is amplified and sent to a detecting meter, and the Y-axis of a cathode ray oscilloscope (the X-axis is connected to the audio oscillator). Resonance is indicated by a deflection of the detection meter and by a Lissajous pattern on the oscilloscope.

Three methods are commonly employed to drive the specimens in flexural vibration.

(a) The specimen is mounted on foam rubber pads at 0.224 L from each end, where L is the specimen length. (These are the node points when the specimen is vibrating at its fundamental flexural frequency.) The driver is then placed directly in contact with the specimen at either the center or at one end.

(b) The specimen is supported as above; however, the driver is placed close to but not touching the specimen. This is known as air gap driving.

(c) The specimen is suspended close to its nodes by wire or other material. One end of the suspension is attached to the driver, and the

other end is fastened to the pick-up.

Methods similar to a and b have been used for driving a specimen in torsion. The specimen is supported at its node for torsional resonance, which is midway between the ends of the bar, and the driver is located at one corner of the specimen.

F. Damping Measurements

1. Damping Relations

The term damping is used to refer to the energy dissipation processes of a material or system under cyclic stress[23]. In most cases a conversion of mechanical energy to heat is involved. A variety of terminology has been used to describe damping; however, almost all descriptions are derived from the linear single degree of freedom system with a viscous damper in parallel with a spring.

One of the most common quantities characterizing damping is the logarithmic decrement. The logarithmic decrement (α) for damped oscillations is the natural logarithm of a ratio of the amplitudes of successive cycles. An expression for the average value for several cycles is given[24] as:

$$\alpha = \frac{1}{n} \ln \frac{A_o}{A_n} , \qquad (6)$$

where n = number of cycles,

A_o = amplitude of vibration for the original cycle, and

A_n = amplitude of vibration after n cycles.

When a specimen is vibrated by an external source and the frequency of the driving mechanism is varied, the amplitude of specimen oscillation will pass through a maximum at the resonant frequency. This is illustrated in Figure 1. Increased damping tends to reduce the

amplitude and broaden the base of this resonance curve. Based on this phenomenon, an expression relating logarithmic decrement to peak width and resonance frequency has been derived. This is given by Jensen[25] as:

$$\alpha = \pi \frac{\Delta f}{f_n} \sqrt{A_x^2/(A_{max}^2 - A_x^2)} \quad , \tag{7}$$

where Δf = the width of the resonance peak at amplitude A_x in cycles per second and

A_{max} = the maximum amplitude at resonance frequency f_n.

By convention it is generally chosen to measure the width of the resonance curve at an amplitude:

$$A_x = 0.707\ A_{max}. \tag{8}$$

Equation 7 then reduces to:

$$\alpha = \pi \frac{\Delta f}{f_n} . \tag{9}$$

At frequencies below resonance, the specimen moves in phase with the driving force and the phase angle (γ) is zero. As the frequency is increased, the vibration of the specimen lags increasingly behind the driving force, until at frequencies above resonance, it is completely out of phase with the driving force. Figure 2 shows how the amplitude A and the phase angle vary across resonance. Smith and Berns[26] have related the phase angle and the resonant frequency to the logarithmic decrement as:

$$\alpha = (f_n/f - f/f_n)\ \pi \tan \gamma, \tag{10}$$

where f = frequency very close to the resonance frequency.

2. Techniques for Measuring Damping

Probably the most widely used method of measuring damping, and certainly the one in longest use, is that of the decay rate of a tor-

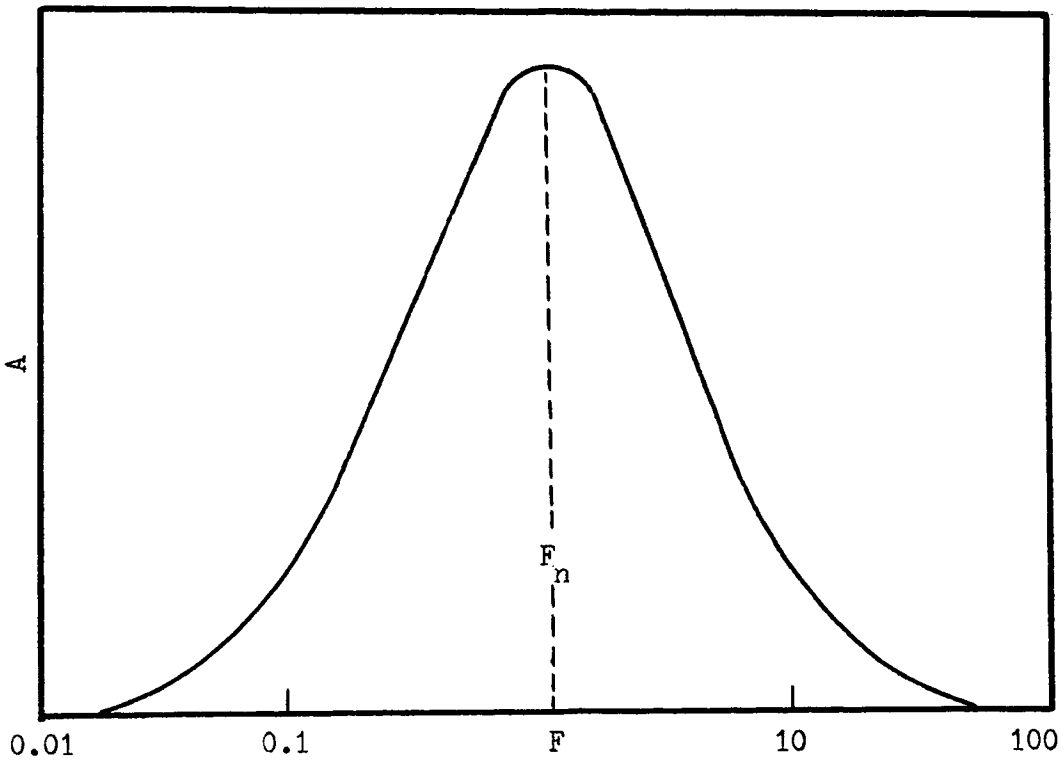

Figure 1. Increase in amplitude across resonance.

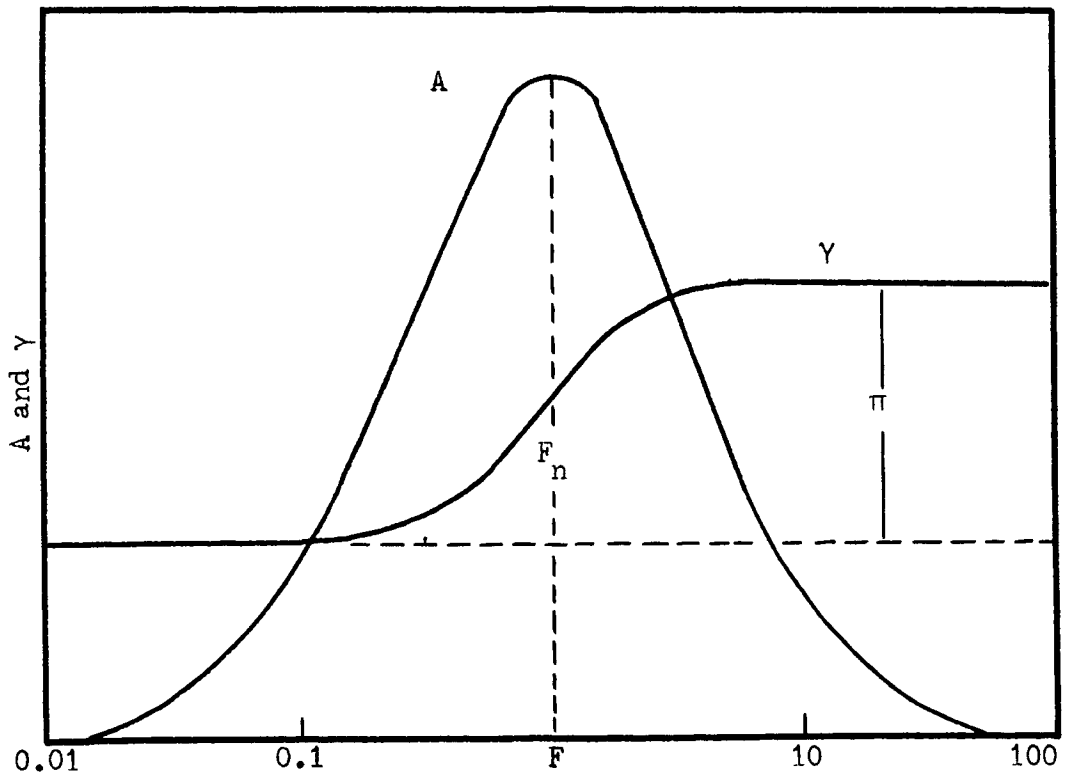

Figure 2. Change in phase angle across resonance.

sion pendulum. By this technique, the logarithmic decrement can be determined by use of equation 6.

Another method widely used[22,27], particularly since it utilizes the same equipment as employed in measuring elastic constants, is the bandwidth method. The specimen is first vibrated at its resonance frequency which is indicated by a maximum scale deflection on the detecting voltmeter or ammeter. The frequency is then varied above resonance to a point where the detection meter registers 0.707 maximum. This is repeated below the resonance frequency. The logarithmic decrement may be calculated by use of equation 9.

The difficulty with the bandwidth method is that the magnitude of the driving force must be constant below resonance, above resonance, and at resonance. This problem has been eliminated by the "frequency-phase"[26] method for measuring the logarithmic decrement. Again, this procedure utilizes the same equipment needed for determining the elastic constants. Details are given in APPENDIX B.

III. EXPERIMENTAL PROCEDURES

A. Batch Materials and Formulation

At the onset of this investigation, it was decided to follow through with the same raw materials as were used in previous work[3] on this system. These raw materials were: potassium silicofluoride (K_2SiF_6) from the U. S. Phosphoric Products Div., Tennessee Corp.; magnesium carbonate (light powder) and potassium carbonate from Fisher Scientific Company; and powdered silica from the Ottawa Flint Company. All materials were -200 mesh particle size.

Raw batch compositions were calculated using equivalents[28]. Preliminary studies on variations in the stoichiometric batch composition indicated that a satisfactory glass-ceramic could be made from a raw batch containing 10 percent batch equivalent excess fluorine. The raw materials, batch equivalents, and constituent percentages are presented in Table I.

TABLE I

Raw Materials, Batch Equivalents, and Constituent Percentages

Raw Material	Batch Equivalent	Percent Constituents After Melting
K_2SiF_6	0.366 F_2	9.704% F_2
	0.122 K_2O	8.018% K_2O
	0.122 SiO_2	5.115% SiO_2
$3MgCO_3 \cdot Mg(OH) \cdot 3H_2O$	0.833 MgO	23.423% MgO
K_2CO_3	0.045 K_2O	2.951% K_2O
SiO_2	1.211 SiO_2	50.781% SiO_2

The raw materials previously listed were weighed in their proper proportions, to the nearest 0.01 gram, on a two pan torsion balance. The batch was then mixed in a Patterson-Kelley twin shell blender for one hour. To prevent batch segregation, the mixed batches were immediately pressed into fifty gram pellets on a hydraulic press. Before melting, the pellets were dried at 500°C for one-half hour.

B. Specimen Formation

All batches were melted in high-silica fireclay crucibles in a top loading furnace heated with silicon carbide resistance elements. The crucibles were preheated at 1300°C for one-half hour prior to being used for melting. After being heated, the crucibles were removed from the furnace, charged with 250 grams of raw batch, and replaced in the furnace at 1300°C. Forty-five minutes were allowed for complete batch melting.

Individual specimens were formed by pouring 25 grams of molten glass into a graphite mold preheated to 500°C. The design of this mold permitted bars approximately 6 inches long by 1 inch wide by 3/16 inch thick to be pressed. After forming, the bars were removed from the mold and annealed in a globar furnace at 500°C.

C. Specimen Grinding

Inasmuch as each test specimen, as removed from the mold, varied in its dimensions, all specimens were ground using -200 mesh silicon carbide abrasive powder on a steel potters wheel. It was possible by this technique to obtain faces and edges parallel to within 0.003 inch along the lengths of test bars.

D. Heat Treatment of Test Specimens

Test specimens were heated in a Harrop electric box furnace. This

furnace allowed three heating rates, designated as "low", "medium", and "high". Only the medium and high rates were used. With these settings, a heating rate as shown in Figure 3 was obtained. Heat treatment temperatures and times are also shown in Figure 3. After the respective heat treatments, the bars were cooled to room temperature in the furnace.

E. Density Measurements

Density measurements were made using Archimedes Principle. Test specimens were first soaked in distilled water, under vacuum, for three to four hours. Submerged weights were then obtained using a Mettler single pan precision balance. The specimens were then dried overnight at approximately 106°C, and reweighed on the Mettler balance to obtain dry weights.

F. Room Temperature Determinations of Elastic Constants

Room temperature measurements of modulus of elasticity, shear modulus, and Poisson's ratio were determined on glass and heat-treated specimens using sonic apparatus marketed by Electro Products Laboratories Inc. This consisted of a Hewlett Packard wide range oscillator used through a power amplifier to drive a Jensen speaker. The response of the test piece was picked up by an Astatic stereo cartridge; the relative intensity of the amplified pick-up output was then indicated on a D. C. microammeter. The input to the driver and the output of the pick-up were fed into a Dumont oscilloscope so that resonant frequencies could be determined by use of Lissajous figures on the cathode ray tube. Resonant frequencies were read from an Ekco counter.

The specimens were suspended from the driver and pick-up with

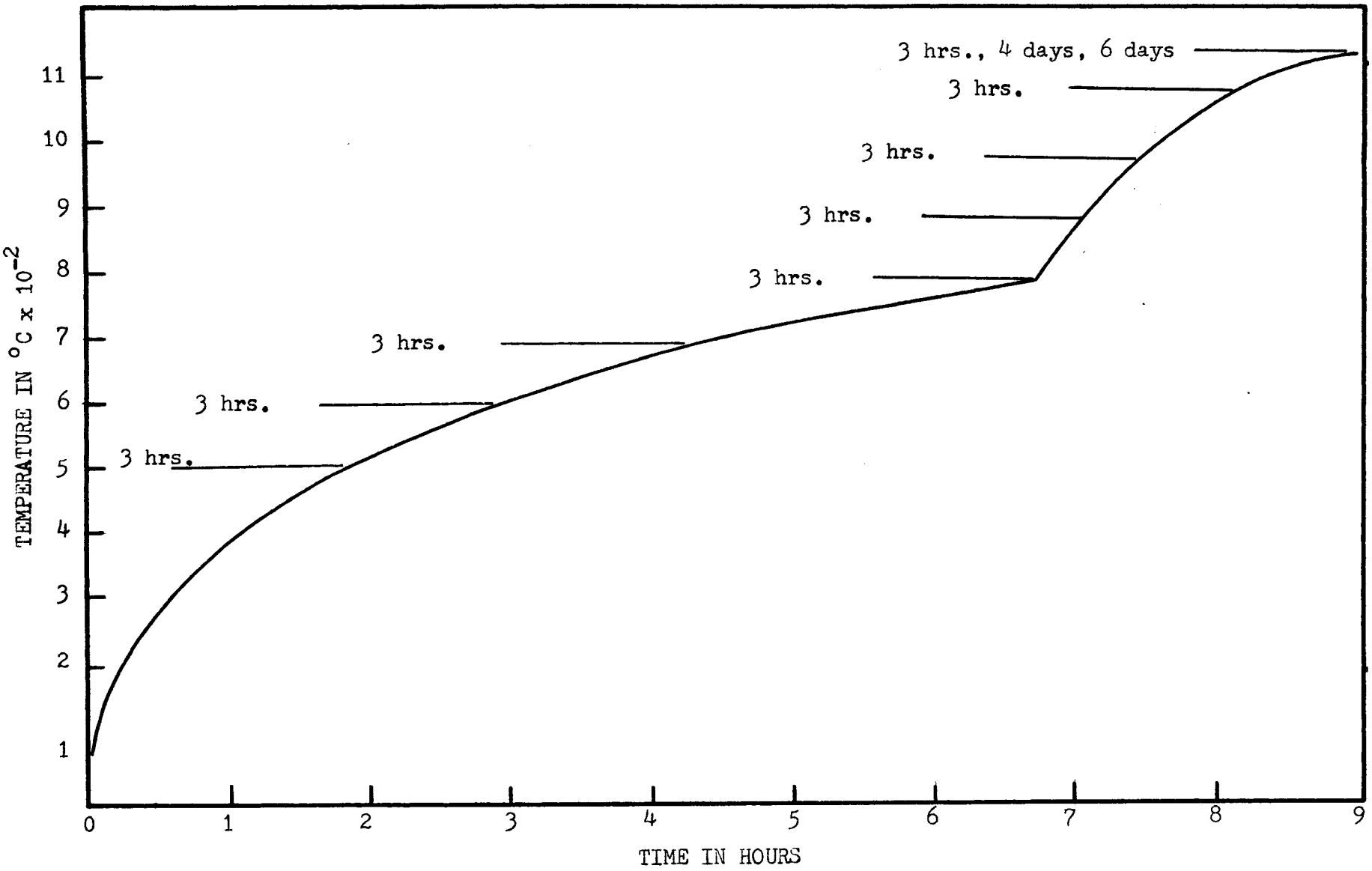

Figure 3. Heat treatment schedule.

nylon thread. For flexural vibration, the threads were secured close to the specimen nodes (0.224 L from each end) as shown in Figure 4. Torsional vibration was induced by suspending the test bars at each end in such a manner as to produce maximum torque; this is shown in Figure 5. The frequency was varied until the microammeter and Lissajous figures indicated the specimen to be vibrating in resonance. The elastic constants were then calculated from the specimen dimensions, mass, and the resonant frequencies with the aid of tables compiled by Hasselman[29].

G. Room Temperature Logarithmic Decrement Determinations

Logarithmic decrement measurements were made at room temperature employing the "frequency-phase" technique developed by Smith and Berns[26]. This method involves the set-up for inducing flexural vibrations as described in the previous section. A more comprehensive account of this procedure is given in Appendix B.

H. Young's Modulus of Elasticity and Logarithmic Decrement at Elevated Temperatures

To follow phase changes at temperature, the modulus of elasticity and logarithmic decrement were determined from room temperature to 800°C employing techniques previously described for room temperature measurements. The driver and pick-up were placed 15 inches above a top-loading bench furnace. A glass bar was then suspended in the furnace from the driver and pick-up using Refrasil refractory yarn produced by the H. I. Thompson Company, Gardena, California. Determinations employing this technique were also made to 625°C and 700°C respectfully with 3 hour holding periods at these temperatures. The heating rate in all determinations was 2°C per minute.

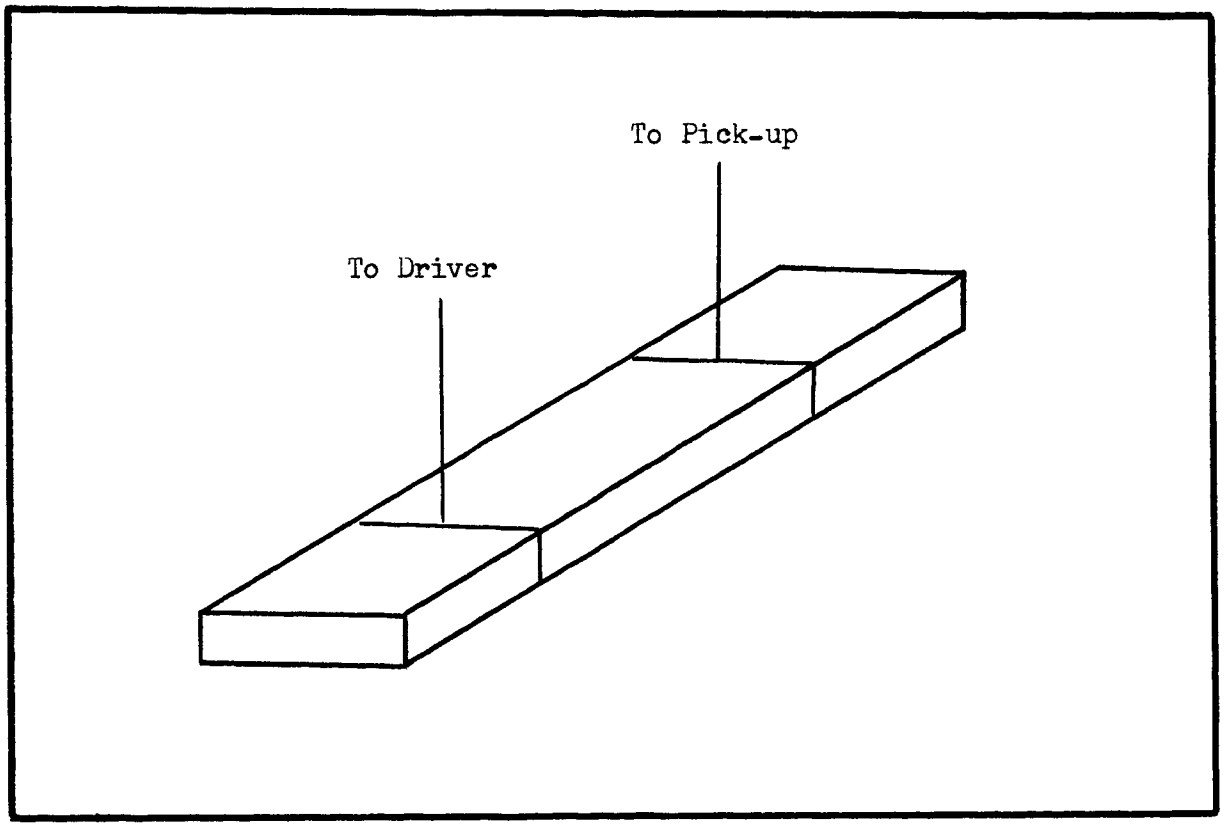

Figure 4. Flexural vibration set-up.

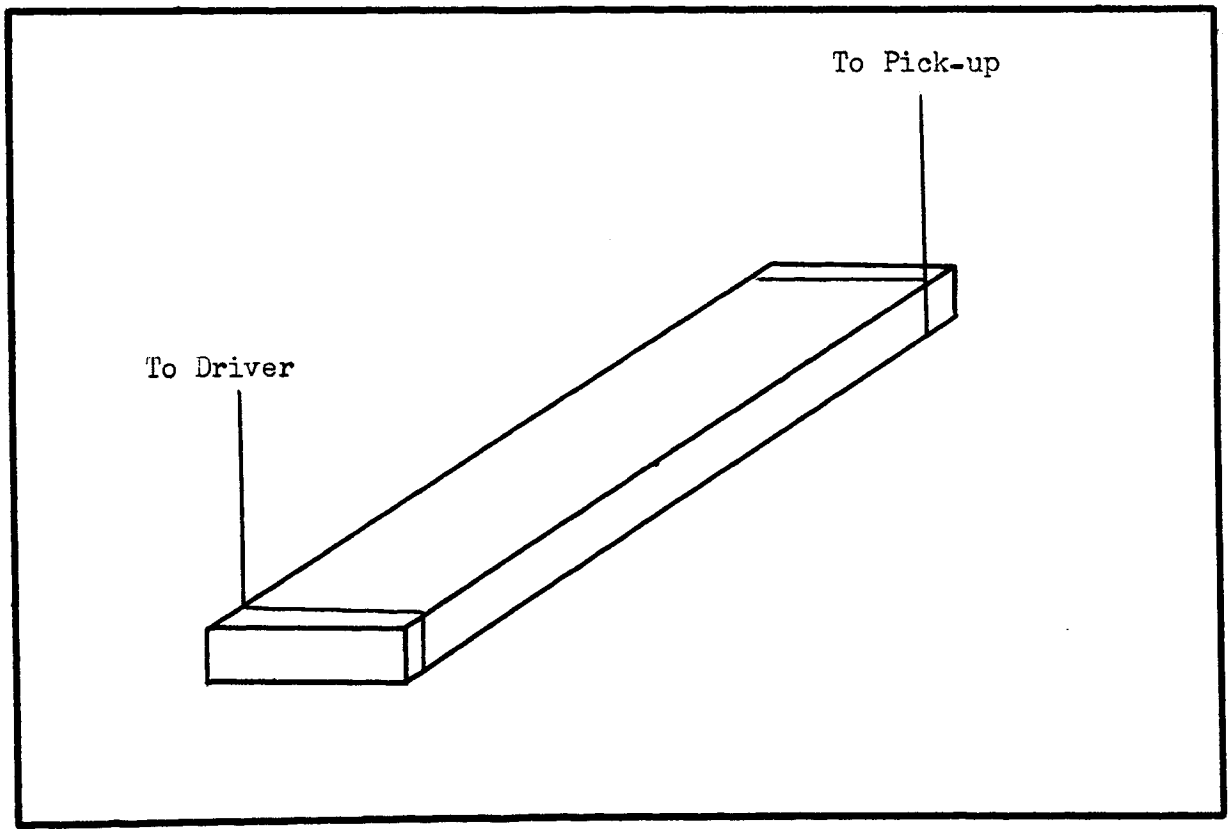

Figure 5. Torsional vibration set-up.

Young's modulus at elevated temperatures was calculated using the relation[29]:

$$E_t = E_o \frac{f_t^2}{f_o^2} \, 1/(1 + \alpha\Delta T), \qquad (11)$$

where E_t = Young's modulus at elevated temperatures,

E_o = Young's modulus at room temperature,

f_t = the resonance frequency at elevated temperatures,

f_o = the resonance frequency at room temperature,

α = the coefficient of linear thermal expansion, and

ΔT = the difference between temperature T and room temperature.

I. Thermal Expansion Determinations

Thermal expansion apparatus consisted of a small tubular, electric furnace, designed to accomodate a fused silica tube dilatometer. This dilatometer is described in the A.S.T.M. standard test C 337-57. Glass test specimens were heated in the dilatometer at a rate of 2°C per minute. Each specimen was held at a selected temperature for three hours.

IV. EXPERIMENTAL RESULTS

A. Appearance of Heat-Treated Specimens

Test specimens heat-treated at 600°C and 700°C respectively were not visibly different from the glass. Heat treatments at 800°C and 900°C produced translucency in the specimens. A completely white specimen having a vitreous luster was produced after heat treatment at 1000°C. Heat treatments above 1000°C produced an opaque white material, and with extended holding times at 1150°C, crystals were observed on fracture surfaces without optical aids. A hard crust was observed on the surface of test specimens heat-treated above 1000°C.

B. Density, Linear Shrinkage, and Weight Loss

Densities, linear shrinkages, and weight losses as determined on heat-treated test specimens are reported in TABLE II. Density changes and shrinkages were not observed in heat treatments below 600°C; however, after a heat treatment at 600°C for three hours, an appreciable density increase was observed. Density and shrinkage reached a maximum after three hour heat treatments at 800°C and 900°C respectively. Heat treatments above 1000°C produced densities and shrinkage lower than the maximum observed at 800°C and 900°C. This is attributed to orientation and growth of mica crystals, resulting in voids.

Weight losses are attributed to fluorine volatilization. These losses were small after heat treatments to 1000°C; however, much greater losses were observed in specimens heat-treated above this temperature.

C. Room Temperature Elastic Constants and Logarithmic Decrement

The elastic constants of test specimens heat-treated between 500°C and 1150°C are presented in TABLE III. Figure 6 is a plot of

TABLE II

Effect of Heat Treatment on Densities, Linear Shrinkage, and Weight Loss

Heat Treatment	Density	Percent Linear Shrinkage	Percent Weight Loss
500°C - 3 hrs.	2.571 ± .001	0	0
600°C - 3 hrs.	2.642 ± .001	0.53 ± .04	0.009 ± .005
700°C - 3 hrs.	2.712 ± .001	1.65 ± .04	0.014 ± .006
800°C - 3 hrs.	2.794 ± .001	2.65 ± .04	0.021 ± .005
900°C - 3 hrs.	2.792 ± .001	3.10 ± .03	0.042 ± .005
1000°C - 3 hrs.	2.781 ± .001	2.40 ± .03	0.089 ± .005
1100°C - 3 hrs.	2.751 ± .001	2.12 ± .03	0.184 ± .005
1150°C - 3 hrs.	2.688 ± .001	0.27* ± .04	0.533 ± .006
1150°C - 4 days	2.672 ± .002	0.74 ± .04	0.618 ± .005
1150°C - 6 days	2.698 ± .001	0.23* ± .03	0.887 ± .006

* expanded

TABLE III

Effect of Heat Treatment on Elastic Constants

Heat Treatment	Young's Modulus x 10^{-6} psi	Shear Modulus x 10^{-6} psi	Poisson's Ratio
500°C - 3 hrs.	11.61 ± .33	4.68 ± .065	.239 ± .039
600°C - 3 hrs.	11.14 ± .24	4.36 ± .051	.277 ± .031
700°C - 3 hrs.	10.42 ± .36	4.19 ± .060	.243 ± .042
800°C - 3 hrs.	10.45 ± .22	4.08 ± .057	.282 ± .030
900°C - 3 hrs.	10.08 ± .20	3.96 ± .052	.273 ± .031
1000°C - 3 hrs.	10.01 ± .23	3.80 ± .050	.313 ± .035
1100°C - 3 hrs.	5.61 ± .09	2.52 ± .032	.114 ± .023
1150°C - 3 hrs.	4.94 ± .07	2.15 ± .033	.111 ± .026
1150°C - 4 days	3.73 ± .06	1.66 ± .025	.115 ± .025
1150°C - 6 days	3.89 ± .06	1.74 ± .028	.120 ± .025

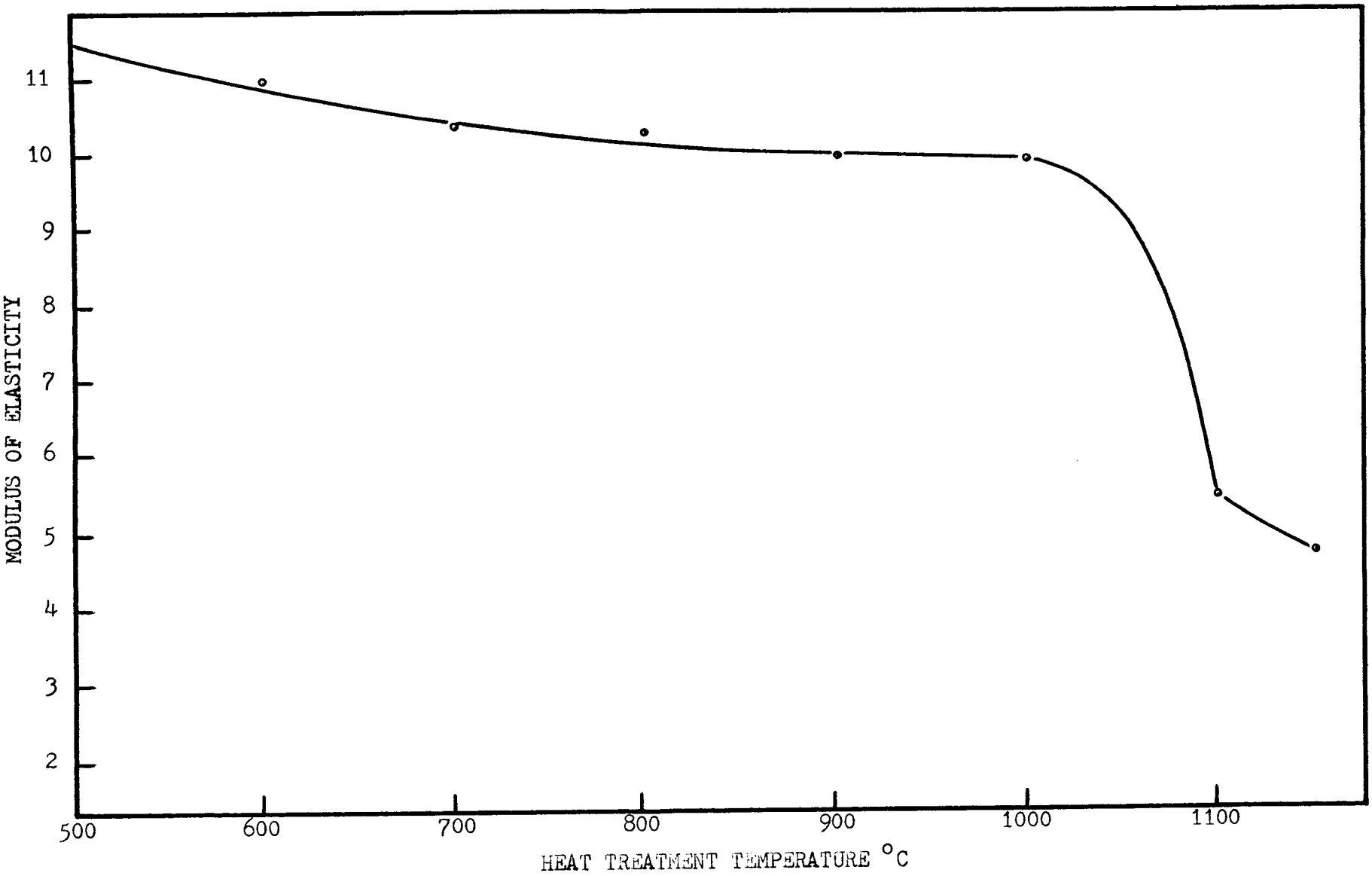

Figure 6. Effect of heat treatment on Young's modulus.

Young's modulus as a function of three hour heat treatments. An initial decrease in the modulus of elasticity and shear modulus is evidenced after heat treatment at 600°C. This data shows a gradual decreasing trend with heat treatments from 600°C to 1000°C. Heat treatments above 1000°C result in much lower values of the elastic constants.

Logarithmic decrement data are given in TABLE IV, and Figure 7 is a plot of the logarithmic decrement as a function of three hour heat treatments. From 600°C to 900°C a decreasing trend is observed. There is a slight increase after a heat treatment at 1000°C; however, a very appreciable increase is seen after heat treatment at 1100°C. This increase corresponds to the decreases seen in the elastic constants.

D. Logarithmic Decrement and Modulus of Elasticity at Elevated Temperatures

Figure 8 is a plot of the logarithmic decrement and the modulus of elasticity as a function of temperature. Close to 600°C, a peak is noted in the logarithmic decrement, and a corresponding discontinuity appears in the modulus of elasticity. This behavior relates to the ordering taking place in this temperature range. A change in slope of the logarithmic decrement curve is also noted immediately preceding this peak.

Beyond 800°C, it became extremely difficult to obtain readings because of low vibration amplitude.

Figure 9 shows plots of the logarithmic decrement as a function of time. Test specimens were heated at a rate of 2°C per minute to their respective holding temperatures, and measurements were started

TABLE IV

Effect of Heat Treatment on Logarithmic Decrement

Heat Treatment	Logarithmic Decrement x 10^3
500°C - 3 hrs.	2.4 ± 0.23
600°C - 3 hrs.	1.3 ± 0.11
700°C - 3 hrs.	1.0 ± 0.09
800°C - 3 hrs.	1.0 ± 0.10
900°C - 3 hrs.	0.8 ± 0.10
1000°C - 3 hrs.	1.6 ± 0.11
1100°C - 3 hrs.	8.8 ± 1.1
1150°C - 3 hrs.	45. ± 3.4
1150°C - 4 days	13. ± 2.0
1150°C - 6 days	17. ± 1.9

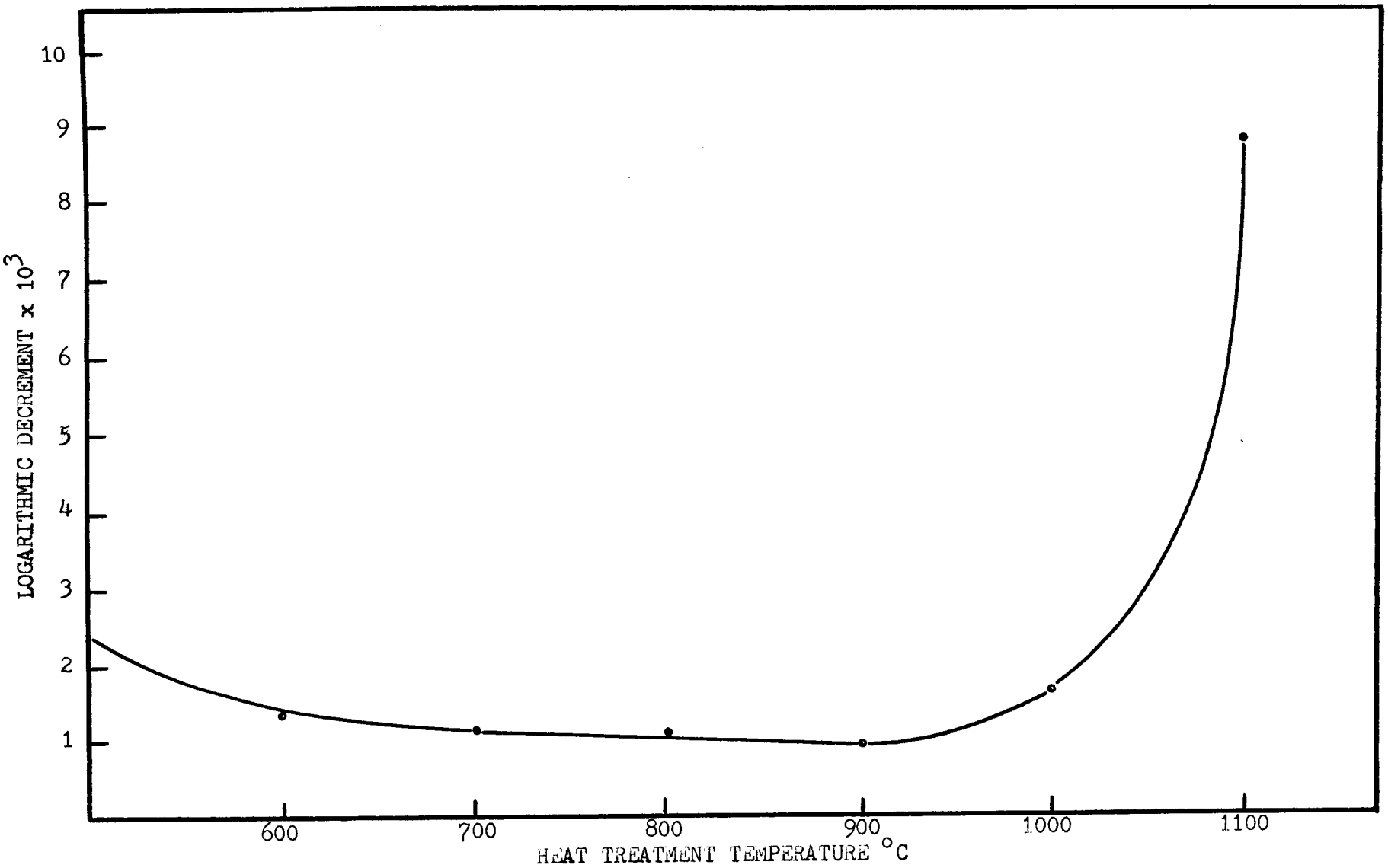

Figure 7. Effect of heat treatment on logarithmic decrement.

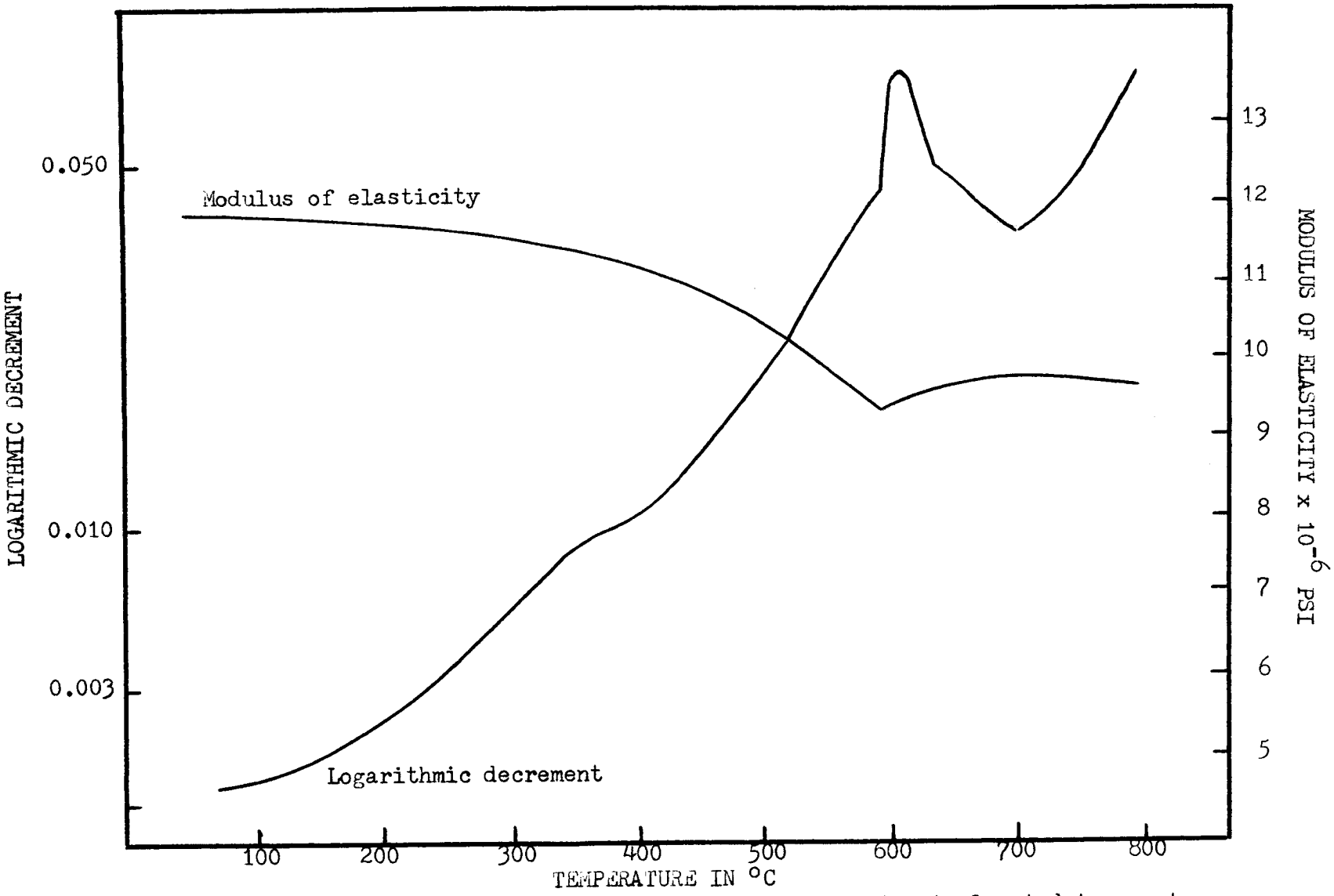

Figure 8. Logarithmic decrement and modulus of elasticity at elevated temperature.

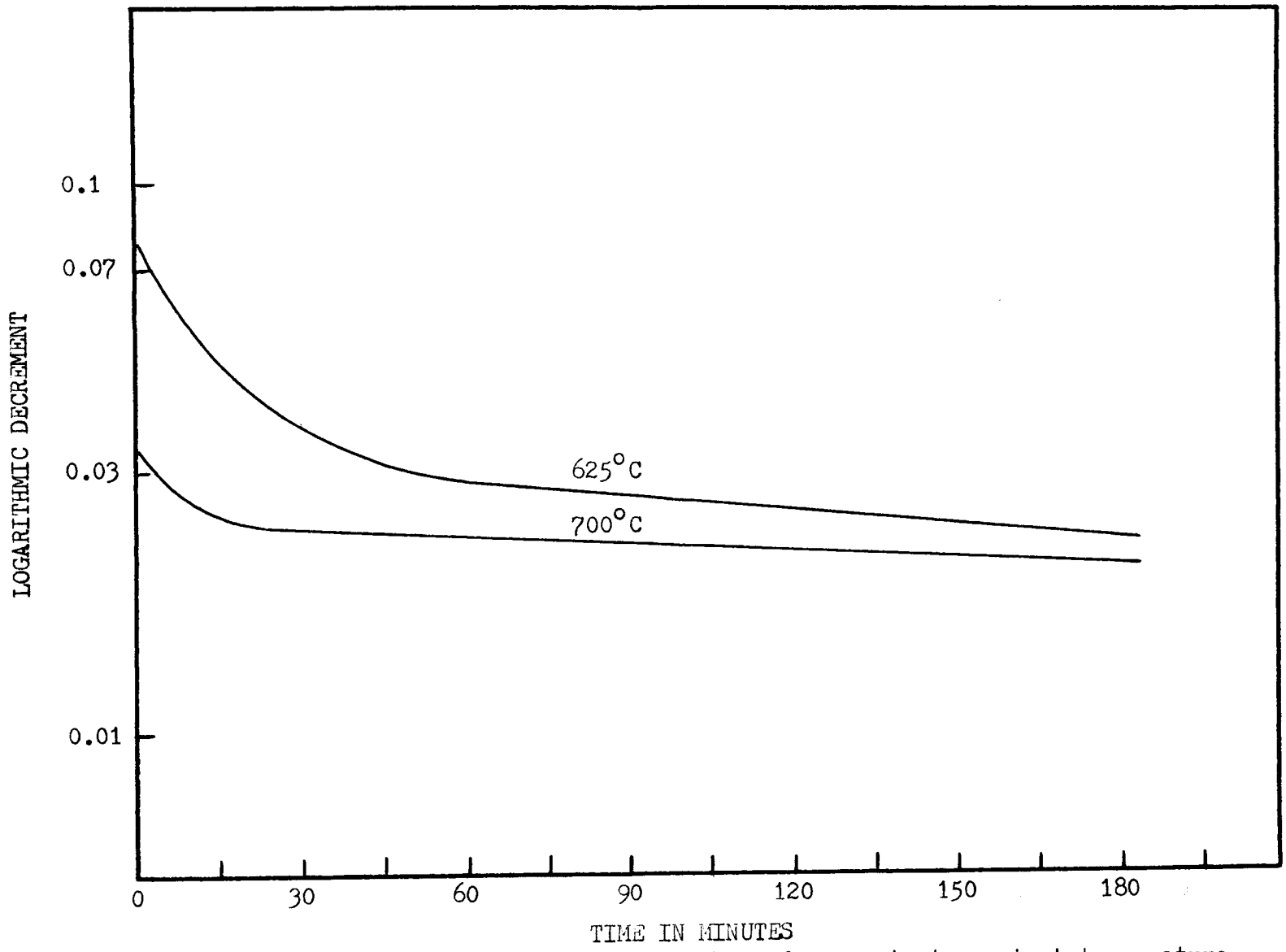

Figure 9. The effect of time on logarithmic decrement at constant temperature.

upon reaching holding temperature. Both curves are seen to decrease with time; the decrease is most severe during the first thirty minutes.

To the author's knowledge, this is the first time the frequency-phase method has been used for determining the logarithmic decrement at elevated temperatures. Therefore, the logarithmic decrement of a tetrasilicic mica glass fiber was determined under vacuum using an inverted torsion pendulum at a constant frequency of 0.4 cycles per sec. This torsion pendulum has been described by Miller[30]. Figure 14 in APPENDIX C shows curves of the logarithmic decrement by the frequency-phase technique and by the torsion pendulum technique. The values obtained by the torsion pendulum are higher than those obtained by the frequency-phase technique; however, the shape of the curves is quite similar.

E. Thermal Expansion Determinations

Thermal expansion of test specimens having received no prior heat treatment is presented in Figure 10. This curve shows the abrupt nature of the transformation from an amorphous to an ordered state. From room temperature to 550°C, the expansion was determined to be 6.89×10^{-6} in./in./°C. A slight discontinuity is observed after 550°C, and rapid shrinkage is noted in the range of 600°C. Shrinkage at 600°C and 675°C as a function of time is presented in Figure 11. The test specimens were heated at a rate of 2°C per minute to their respective holding temperature, and time zero indicates the time at which holding temperature is reached. The shrinkage rate is seen to decrease with time and temperature.

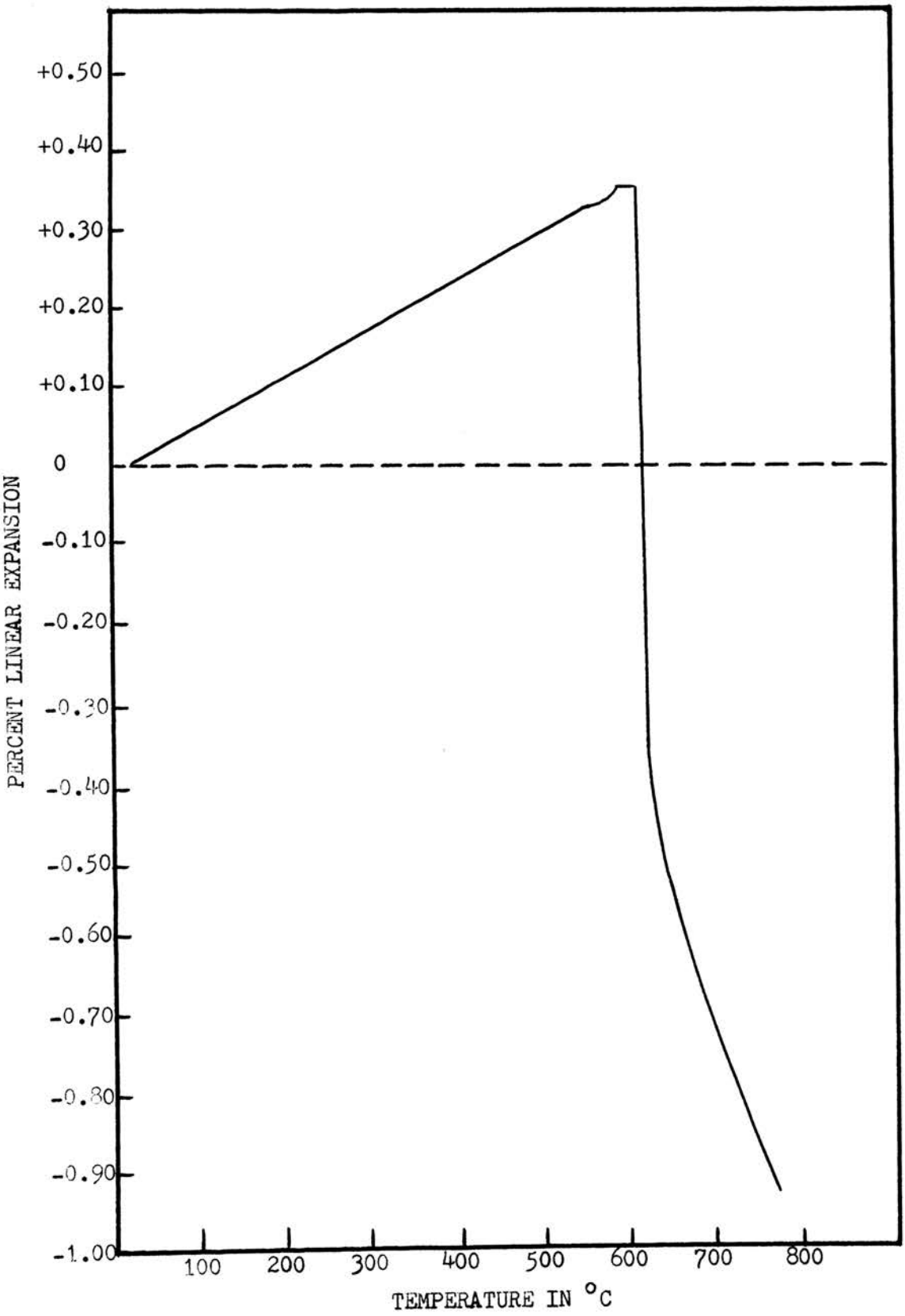

Figure 10. Thermal expansion of tetrasilicic mica glass.

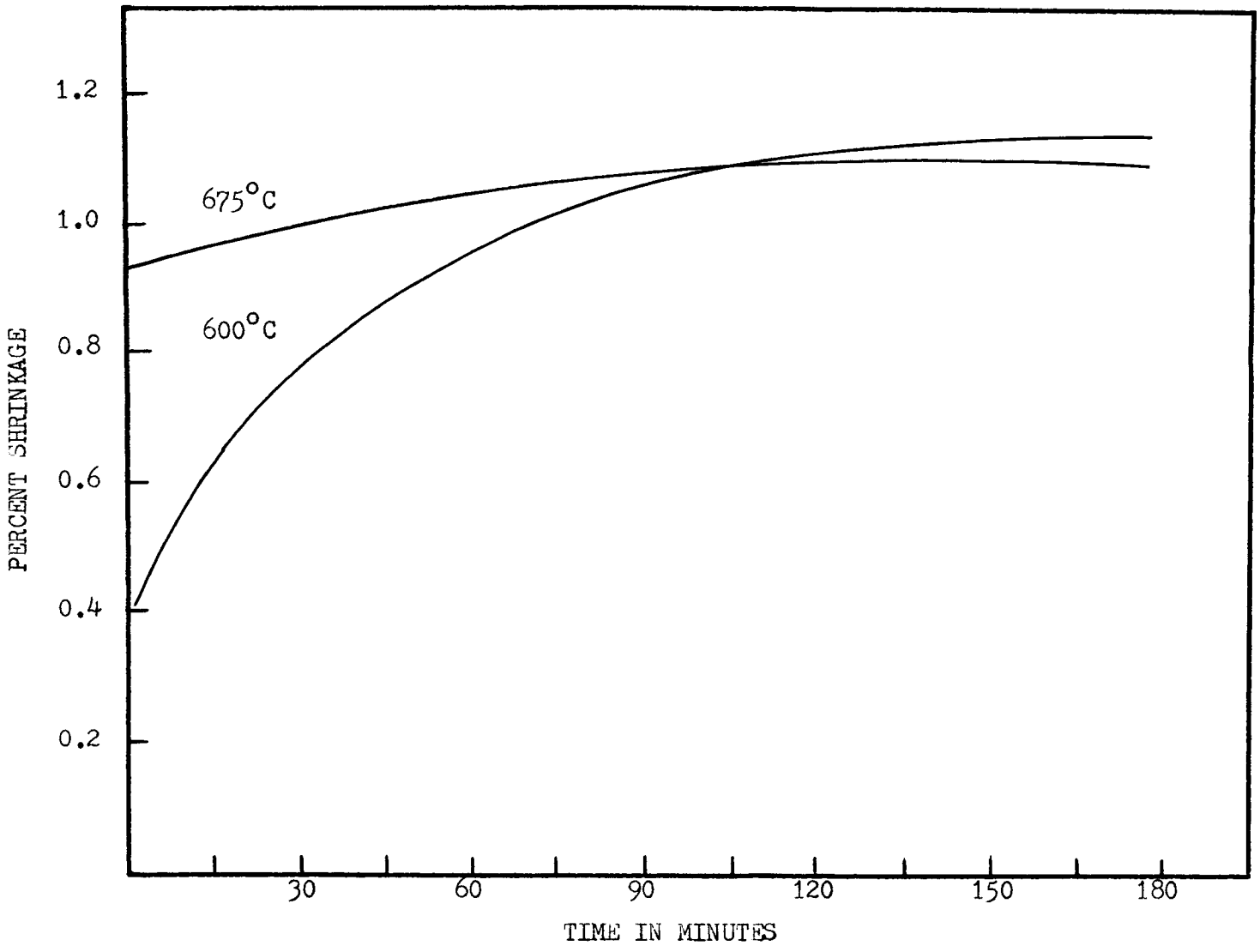

Figure 11. Shrinkage rate at holding temperatures.

V. DISCUSSION OF RESULTS

A. Review of X-Ray Diffraction Data

X-ray diffraction was employed by Schumacher[31] to follow the development of tetrasilicic mica. Diffraction patterns of specimens heat-treated at 700°C showed a number of broad peaks with d-spacings shifted slightly from those of tetrasilicic mica. These peaks were related to a pseudocrystalline phase. Heat treatment at 800°C, however, produced an increase in the number and intensity of peaks. Furthermore, the d-spacings corresponded to those of mica. This was felt to be indicative of mica crystal formation. Heat treatments at higher temperatures and longer times resulted in further increases in peak heights until a fully devitrified mica was produced after a six day holding period at 1150°C.

A review of this diffraction data indicates that there is a significant increase in the intensities of the major mica peaks after a heat treatment at 1100°C for three hours. This is indicative of appreciably increased mica growth.

B. Specimen Appearance

The glass-like appearance of test specimens heat-treated at 600°C and 700°C shows the very small grain size associated with the pseudo-crystalline phase. The translucent appearance of specimens heat-treated at 800°C, 900°C, and 1000°C is indicative of small-grained mica formation. The low intensities of x-ray diffraction peaks suggest particle sizes to be less than 1000 A. Increasing crystal sizes are evidenced by the opacity of specimens heat-treated at 1100°C, and the abundance of crystals visually observed after 6 days at 1150°C clearly shows a high degree of tetrasilicic mica content.

The crusty surface observed in higher temperature heat treatments is associated with fluorine decomposition.

C. Density, Linear Shrinkage, and Weight Loss

Phase developement is seen by density changes and shrinkage. The appreciable density increase and shrinkage after heat treatment at 600°C is associated with the pseudocrystalline phase. The densities after heat treatments at 800°C, 900°C, and 1000°C are approaching the theoretical density of tetrasilicic mica, i.e., 2.835 gm./cc. This suggests high tetrasilicic mica content. The lower densities of specimens heat-treated above 1000°C show evidence of bloating. This parallels the increased mica growth evidenced from x-ray diffraction. The increased mica growth and subsequent reorientation introduce voids in the structure.

Low fluorine losses are noted with heat treatments below 1000°C; thus the chemical composition is probably not greatly affected. The comparatively high losses noted with heat treatments at 1150°C could have an appreciable effect on dielectric and physical properties. The crusty appearance noted on the outer surface of test specimens would suggest a majority of the loss to be occurring close to the surface.

D. Logarithmic Decrement and Elastic Constants at Room Temperature

The development of the pseudocrystalline phase and/or tetrasilicic mica with heat treatments from 600°C to 1000°C is reflected in the gradual decreasing trend in the modulus of elasticity and shear modulus. The appreciable modulus decreases after heat treatment at 1100°C denote voids and increased grain size resulting from increases in mica growth. This is in good agreement with x-ray

diffraction and density measurements.

The decreases in logarithmic decrement correspond to those of the elastic constants with heat treatments to 900°C. The slight increases after heat treatment at 1000°C could be indicative of grain boundary interactions. The significant increase in logarithmic decrement after heat treatments at 1100°C and 1150°C again reflects the growth and orientation of mica crystals.

E. Logarithmic Decrement and Modulus of Elasticity at Elevated Temperatures

The peak in the logarithmic decrement and the corresponding discontinuity in the modulus of elasticity are clearly indicative of the transformation to an ordered structure, previously referred to as a pseudocrystalline phase. The sensitivity of the logarithmic decrement is seen from the slope change prior to the transformation peak. This change suggests a preliminary reaction related to the transformation.

X-ray diffraction of samples heat-treated at 800°C indicated possible formation of the tetrasilicic mica from the pseudocrystalline phase. This formation could not be further established from the logarithmic decrement or modulus of elasticity.

The decreasing trend in logarithmic decrement with time at holding temperatures 625°C and 700°C show the rate of phase development to be greater at the lower temperature. Results relative to this were also observed from thermal expansion determinations. A discussion of this will therefore be reserved for the section on thermal expansion.

F. Thermal Expansion

The abrupt shrinkage at 600°C as indicated by thermal expansion is further evidence that the transformation is to a pseudocrystalline

phase. Stookey[9] has stated that it is not uncommon to discover new phases in glass-ceramics, and that some of these are metastable phases whose nucleation and crystallization rates are faster than those of the equilibrium phase. The rate of phase development in the present system, as evidenced by the shrinkage rate, is quite high at 600°C during the first hour. Further development appears to be dependent on higher temperatures; however, as seen from Figure 11, the rate is much lower at 675°C.

The discontinuity in expansion at 550°C would appear to be related to the slope change noted in the logarithmic decrement curve at that temperature. The cause of this behavior is unknown; however, it seems feasible that there could be an alignment of certain ions in the glass prior to the actual transformation.

VI. SUMMARY AND CONCLUSIONS

The crystallization of a tetrasilicic fluor-mica glass was followed through changes in physical properties. Specimens were heat-treated at temperatures from 500°C to 1150°C. The first phase development evidenced by physical property changes occurred after heat treatment at 600°C. This initial phase is a pseudocrystalline phase as indicated by x-ray diffraction. Increasing pseudocrystalline and mica development was noted through increased densities and decreases in the elastic constants and logarithmic decrement with heat treatments to 1000°C. High densities after heat treatments at 800°C, 900°C, and 1000°C indicated a high mica content. Appreciable structural changes were noted with heat treatments above 1000°C. This was attributed to increased growth of tetrasilicic mica.

A peak observed in the logarithmic decrement curve at 600°C established the transformation temperature. Moreover, a change in the slope of the logarithmic curve prior to this peak suggested an ionic arrangement to be occurring prior to the actual transformation. These observations were substantiated by thermal expansion data.

The following conclusions were drawn from this investigation:

1. Rapid transformation of the glass to an ordered structure occurs at 600°C.

2. Heat treatments from 600°C to 1000°C produce an extremely fine-grained glass-ceramic. Significant changes in elastic and anelastic properties after heat treatments above 1000°C are the result of increased tetrasilicic mica growth.

3. Logarithmic decrement measurements of glass specimens by the frequency-phase method at elevated temperatures has proven to be

an extremely sensitive experimental tool for detecting structural changes.

VII. RECOMMENDATIONS FOR FUTURE STUDY

The following recommendations are made for future study:

1. The existence of a pseudocrystalline phase could be more firmly established using electron micrograph studies. Studies such as this might also be helpful in determining the temperature at which tetrasilicic mica first appears.

2. Experiments should be conducted involving the study of additions to the glass which might suppress the rapid formation of the pseudocrystalline phase and permit a transformation from glass to mica.

3. An investigation of the behavior exhibited prior to the transformation would be most interesting and could lead to a better understanding of the kinetics of this system.

BIBLIOGRAPHY

1 R. A. Hatch, R. A. Humphrey, W. Eitel, and J. E. Comeforo, "Synthetic Mica Investigations IX: Reveiw of Progress from 1947 to 1955," U. S. Dept. of Interior, Bur. Mines Invest. No. 5337.

2 F. P. H. Chen, "Kinetic Studies of Crystallization of Synthetic Mica Glass," J. Am. Ceram. Soc., 46 (10) 476-84 (1963).

3 J. J. Tuzzeo, Development of a Fluor-Mica Dielectric Using Glass-Ceramics Fabrication Methods, Master of Science Thesis, Missouri School of Mines and Metallurgy (1964). 71pp.

4 E. S. Dana, A Textbook of Mineralogy, 4th ed., John Wiley and Sons, Inc., (1964). 851pp.

5 A. N. Winchell, "Studies in the Mica Group - Part I," Am. J. Sci., 9 (5) 309-27 (1925).

6 A. N. Winchell, "Studies in the Mica Group - Part II," Am. J. Sci., 9 (5) 415-30 (1925).

7 L. Pauling, "The Structure of Micas and Related Minerals," Nat. Acad. Sci. Pro., 16 (2) 123-29 (1930).

8 R. E. Stevens, "A System for Calculating Analysis of Micas and Related Minerals to End Member," Geol. Surv. Bull. No. 950, pp. 101-19.

9 S. D. Stookey, "Ceramics Made by Nucleation of Glass - Comparison of Micro Structure and Properties With Sintered Ceramics," in Symposium on Nucleation and Crystallization in Glasses and Melts, pp. 1-4. J. Am. Ceram. Soc., 1962.

10 S. D. Stookey and R. D. Maurer, "Catalyzed Crystallization of Glass - Theory and Practice," pp. 78-101, Progress in Ceramic Science, Vol. 2, Pergammon Press, New York, Oxford, London, Paris, 1962.

11 S. D. Stookey, "Catalyzed Crystallization of Glass in Theory and Practice," Ind. Eng. Chem., 51 (7) 805-08 (1959).

12 W. B. Hillig, "A Theoretical and Experimental Investigation of Nucleation Leading to Uniform Crystallization of Glass," in Symposium on Nucleation and Crystallization in Glasses and Melts, pp. 77-89. J. Am. Ceram. Soc., 1962.

13 S. M. Ohlberg, H. R. Golob, J. J. Hammel, and R. R. Lewchuk, "Noncrystalline Microphase Separation in Soda-Lime-Silica Glass," J. Am. Ceram. Soc., 48 (6) 331-32 (1965).

14 Lord Rayleigh, Theory of Sound, 2nd ed., Vol. I, p. 255, Dover Publications, New York, 1945.

15 S. Timoshenko, "On the Transverse Vibrations of Bars of Uniform Cross Section," Phil. Mag., Series 6, 43 (1-6) 125-31 (1922).

16 W. P. Mason, "Motion of a Bar Vibrating in Flexure, Including the Effect of Rotary and Lateral Inertia," J., Acoustical Soc. Am., 6 (4) 246 (1935).

17 W. T. Thomson, "Effect of Rotary and Lateral Inertia on Flexural Vibration of Prismatic Bars," J., Acoustical Soc. Am., 11 (10) 198 (1939).

18 G. Pickett, "Equations for Computing Elastic Constants From Flexural and Torsional Resonant Frequencies of Vibration of Prisms and Cylinders," Proc. ASTM, 45, 846-65 (1945).

19 S. Spinner, T. W. Reichard, and T. E. Tefft, "A Comparison of Experimental and Theoretical Relations Between Young's Modulus and the Flexural and Longitudinal Resonance Frequencies of Uniform Bars," J. Res. Natl. Bur. Std., 64A No. 2 (3-4) 147-55 (1960).

20 T. A. Willmore, R. S. Denginkolb, R. H. Herron, and A. V. Allen, "Application of Sonic Moduli of Elasticity and Rigidity to Testing Heavy Refractories," J. Am. Ceram. Soc., 37 (10) 445-57 (1954).

21 S. Spinner, "Elastic Moduli of Glasses by a Dynamic Method," J. Am. Ceram. Soc., 37 (5) 229-34 (1954).

22 L. Obert and W. I. Duvall, "Discussion of Dynamic Methods of Testing Concrete With Suggestions for Standardization," Proc. ASTM, 41, 1053-71 (1941).

23 B. J. Lazan, "Energy Dissipation Mechanisms in Structures With Particular Reference to Material Damping," A Colloquim on Structural Damping, Am. Soc. Mech. Eng., pp. 1-34, Structural Damping, 1959.

24 R. Plunkett, "Measurement of Damping," Am. Soc. Mech. Eng., pp. 118-31, Structural Damping, 1959.

25 J. N. Jensen, "Damping Capacity....Its Measurement and Significance," U. S. Dept. of Interior, Bur. Mines Invest. No. 5441.

26 G. M. Smith and H. D. Berns, "Frequency-Phase Method for Measuring Material Damping," Mat. Res. Std., 4 (6) 225-27 (1964).

27 D. H. Chung, Elastic and Anelastic Properties of Fine-Grained Polycrystalline Alumina at Elevated Temperatures, Master of Science Thesis, State University of New York College of Ceramics at Alfred University (1960). 87pp.

28 A. I. Andrews, Ceramic Tests and Calculations, John Wiley and Sons, Inc., New York (1955). 172pp.

29 D. P. H. Hasselman, Tables for the Conputation of the Shear

Modulus and Young's Modulus of Elasticity from the Resonant Frequencies of Rectangular Prisms, Applied Research Branch, Research and Development Division, The Carborundum Company, Niagara Falls, New York (1961). 195pp.

30 T. F. Miller, An Instrument for the Measurement of Anelastic Properties of Glass, Master of Science Thesis, University of Missouri at Rolla (1965). 66pp.

31 R. F. Schumacher, The Dielectric Properties of a Synthetic Fluor-Mica Formed by Glass-Ceramic Fabrication Techniques, Master of Science Thesis, University of Missouri at Rolla (1965). 51pp.

APPENDIX A

SHEAR AND ROTARY INERTIA CORRECTION FACTORS FOR DETERMINING YOUNG'S MODULUS OF ELASTICITY

A. Correction Factors after Pickett[18].

1. For u = 0,

$$T = 1 + 79.02(k/L)^2 - \frac{1201(k/L)^4}{1 + 76.06(k/L)^2} - 125(k/L)^4.$$

2. For u = 1/6,

$$T = 1 + 81.79(k/L)^2 - \frac{1314(k/L)^4}{1 + 81.09(k/L)^2} - 125(k/L)^4.$$

3. For u = 1/3,

$$T = 1 + 88.12(k/L)^2 - \frac{1572(k/L)^4}{1 + 92.61(k/L)^2} - 125(k/L)^4.$$

B. Correction Factor for all values of u after Spinner, Reichard, and Tefft[19].

$$T = 1 + 79.02(1 + 0.0752u + 0.8109u^2)(k/L)^2 - 125(k/L)^4 - \frac{1201(1 + 0.2023u + 2.173u^2)(k/L)^2}{1 + 76.06(1 + 0.14081u + 1.536u^2)(k/L)^2}.$$

In the above equations, u denotes Poisson's ratio.

APPENDIX B

FREQUENCY-PHASE METHOD FOR DETERMINATION OF DAMPING

The general test set-up for the frequency-phase determinations of the logarithmic decrement is shown in Figure 12.

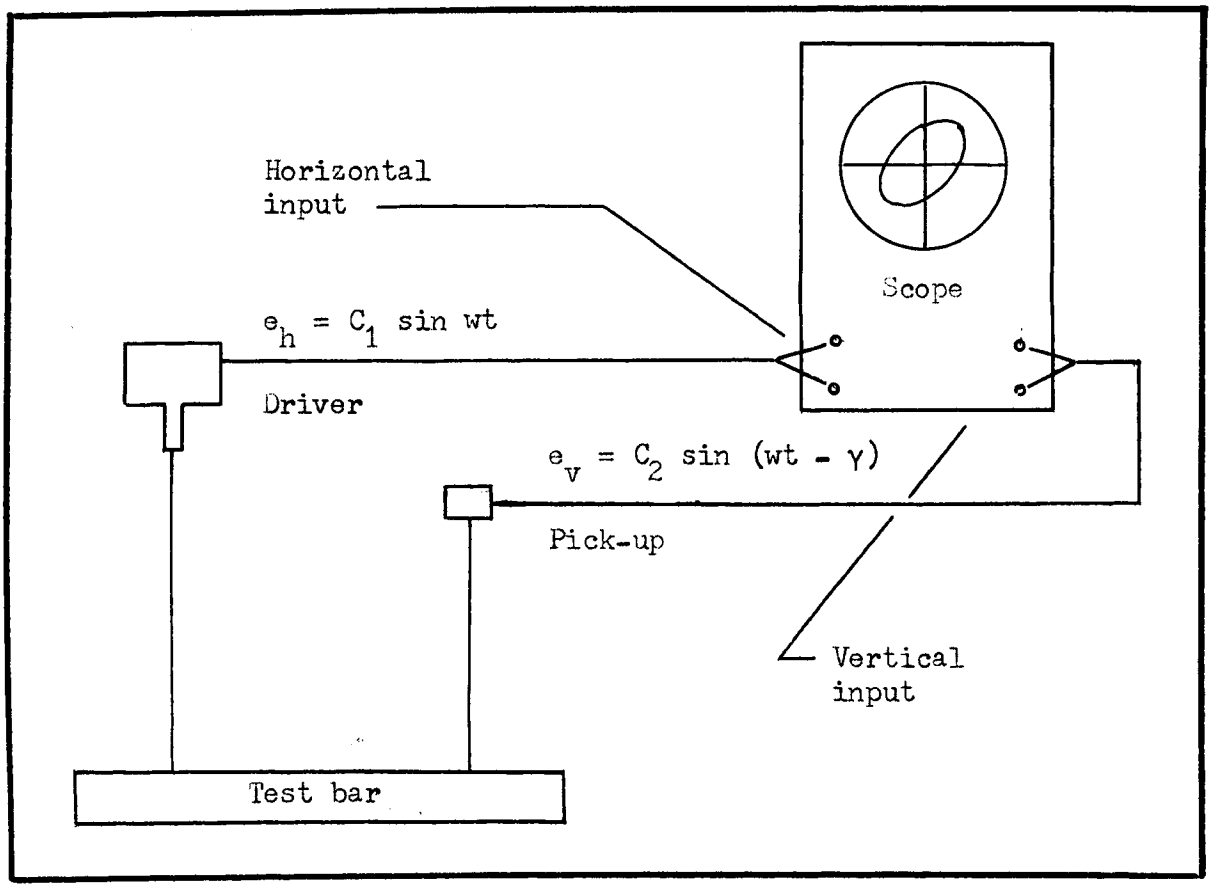

Figure 12. Frequency-phase set-up.

The input voltages to the oscilloscope are:

$$e_h = C_1 \sin wt \qquad \text{horizontal input,} \qquad (1)$$

$$e_v = C_2 \sin(wt - \gamma) \qquad \text{vertical input,} \qquad (2)$$

where C_1 and C_2 are the amplitudes of the horizontal and vertical inputs respectively.

At resonance, the output of the crystal pick-up is 90 degrees ($\pi/2$) out of phase with the output of the driver and the Lissajous pattern on the oscilloscope is vertical as shown in Figure 13a. If

the exciting frequency of the driver (f) is changed slightly, the Lissajous figure is changed slightly as shown in Figure 13b. From

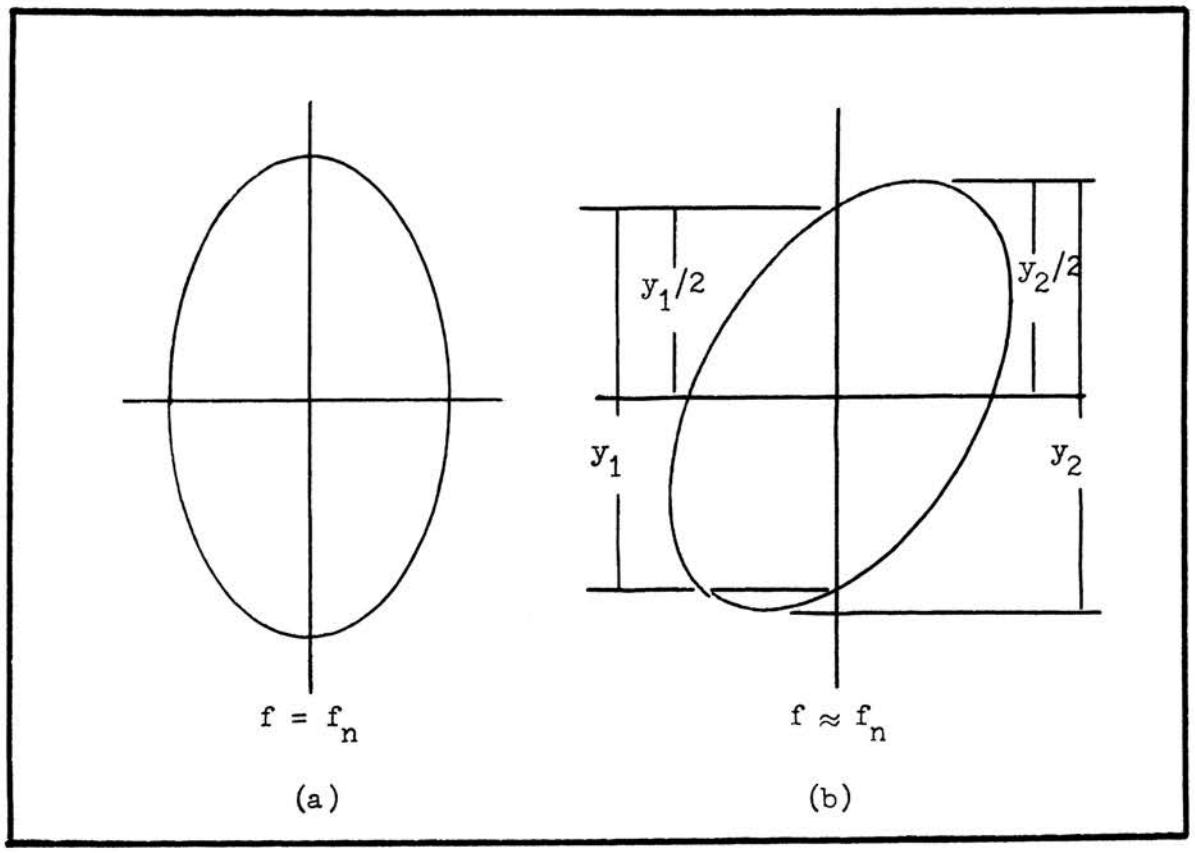

Figure 13. Lissajous figures on scope.

Figure 13b and equations 1 and 2, it is apparent that when wt = 0, or multiples of π, the distance $y_1/2$ is:

$$y_1/2 = e_v = C_2 \sin(-\gamma). \tag{3}$$

Likewise, when wt - γ is $\pi/2$ or odd multiples, the distance $y_2/2$ is:

$$y_2/2 = C_2. \tag{4}$$

From equations 3 and 4, the absolute value for sin γ is found to be:

$$\sin \gamma = \frac{y_1/2}{C_2} = \frac{y_1}{y_2} \qquad \text{or} \qquad \gamma = \sin^{-1} \frac{y_1}{y_2}. \tag{5}$$

The tan γ may be determined from equation 5, and the logarithmic decrement may be computed by use of:

$$\alpha = (f_n/f - f/f_n)\pi \tan \gamma. \qquad (6)$$

The natural frequency, f_n, is first determined by adjusting the frequency of the oscillator until the Lissajous figure is vertical. The oscillator frequency is then changed to a frequency, f, so the ellipse is tilted; at this frequency, the distance y_1 and y_2 are measured. Because very accurate determinations of frequency are necessary, the output of the oscillator is fed to an electronic frequency counter.

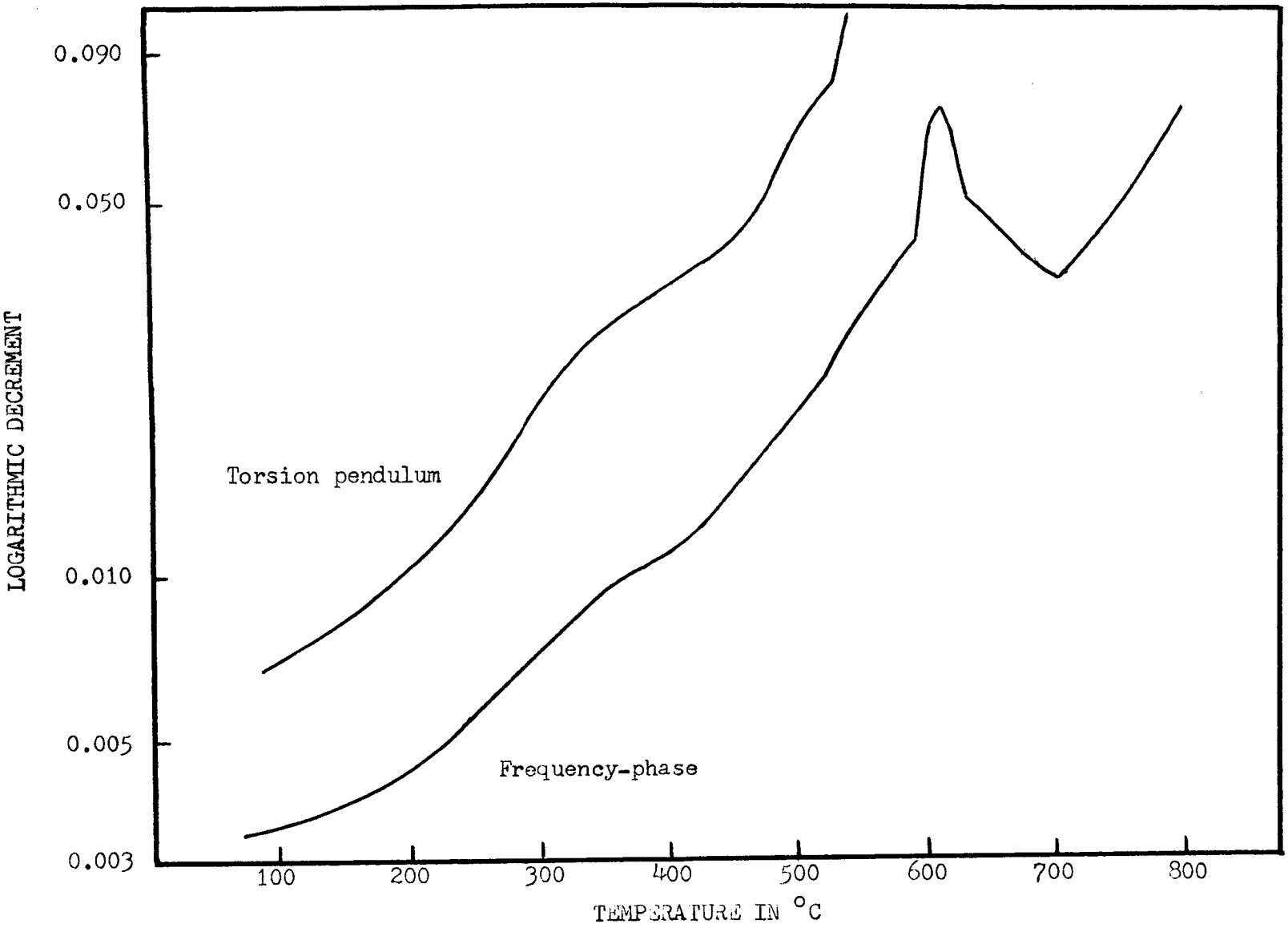

Figure 14. Comparison of results from torsion pendulum and frequency-phase method.

VITA

John Homer Ainsworth was born in McKeesport, Pennsylvania on July 12, 1941. After receiving elementary school training at the Delmont public school, he attended Greensburg High School, and graduated from Franklin Area Joint High School in 1959.

In September 1959, he entered the University of Missouri, School of Mines and Metallurgy where he studied Ceramic Engineering. He received the Bachelor of Science Degree in Ceramic Engineering in May 1963.

From June 1963 to June 1964 he worked as a research engineer in the Technical Center at Ferro Corporation, Cleveland, Ohio.

In June 1964 he entered the Graduate School of the University of Missouri at Rolla as a Research Fellow sponsored by Litton Company.

He is a member of the American Society for Testing and Materials, the American Ceramic Society, and Keramos.